

preceding  $\text{Ca}^{2+}$  release into the lumen of the vesicles.

# ACKNOWLEDGMENTS

We thank Rudene DiCarlo for her expert technical assistance and Dr. Alexander J. Murphy for the use of his computer programs to fit nonlinear regression algorithms to binding data.

# REFERENCES

- Anderson, J. P., Moller, J. V., & Jorgensen, P. L. (1982) *J. Biol. Chem.* 257, 8300-8307.
- Anderson, K. W., & Murphy, A. J. (1983) *J. Biol. Chem.* 258, 14276-14278.
- Anderson, K. W., Coll, R. J., & Murphy, A. J. (1984) *J. Biol. Chem.* 259, 11487-11490.
- Bevington, P. R. (1969) *Data Reduction and Error Analysis for the Physical Sciences*, McGraw-Hill, New York.
- Bishop, J. E., Al-Shawi, M. K., & Inesi, G. (1987) *Biochemistry* 26, 4650-4663.
- Cable, M. B., Feher, J. J., & Briggs, F. N. (1985) *Biochemistry* 24, 5612-5619.
- Champeil, P., & Guillain, F. (1986) *Biochemistry* 25, 7623-7633.
- Coll, R. J., & Murphy, A. J. (1985) *FEBS Lett.* 187, 131-134.
- Coll, R. J., & Murphy, A. J. (1986) *Biochem. Biophys. Res. Commun.* 138, 652-658.
- Crowder, M. S., & Cooke, R. (1987) *J. Biophys. Soc.* 51, 323-333.
- de Meis, L., & de Mello, M. C. (1973) *J. Biol. Chem.* 248, 3691-3701.
- Dupont, Y. (1977) *Eur. J. Biochem.* 72, 185-190.
- Dupont, Y., Pugeois, R., Ronjat, M., & Verjovski-Almeida, S. (1985) *J. Biol. Chem.* 260, 7241-7249.

- Elter, S., & Inesi, G. (1972) *Biochim. Biophys. Acta* 282, 174-179.
- Gould, G. W., East, J. M., Froud, R. J., McWhirter, J. M., Stefanova, H. I., & Lee, A. G. (1986) *Biochem. J.* 237, 217-227.
- Highsmith, S., & Murphy, A. J. (1984) *J. Biol. Chem.* 259, 14651-14656.
- Inesi, G., Goodman, J. J., & Watanabe, S. (1967) *J. Biol. Chem.* 242, 4637-4643.
- Jeng, S. J., & Guillory, R. J. (1975) *J. Supramol. Struct.* 3, 448-468.
- Lacapere, J. J., & Guillain, F. (1988) *Biophys. J.* 53, 338a.
- Lowry, O., Roebrough, N., Farr, A., & Randall, R. (1951) *J. Biol. Chem.* 193, 265-275.
- McIntosh, D. B., & Boyer, P. D. (1983) *Biochemistry* 22, 2867-2875.
- Moller, J. V., Lind, K. E., & Andersen, J. P. (1980) *J. Biol. Chem.* 255, 1912-1920.
- Murphy, A. J. (1981) *J. Biol. Chem.* 256, 12046-12050.
- Nakamura, Y., Kurzmack, M., & Inesi, G. (1986) *J. Biol. Chem.* 261, 3090-3097.
- Neet, K. E., & Green, N. M. (1977) *Arch. Biochem. Biophys.* 178, 588-597.
- Pick, U., & Karlisch, S. J. D. (1980) *Biochim. Biophys. Acta* 626, 255-261.
- Taylor, J. S., & Hatten, D. (1979) *J. Biol. Chem.* 254, 4402-4407.
- Verjovski-Almeida, S., & Inesi, G. (1979) *J. Biol. Chem.* 254, 18-21.
- Yamamoto, T., & Tonamura, Y. (1967) *J. Biochem. (Tokyo)* 62, 558-575.

## Isotope Effect Studies of the Pyridoxal 5'-Phosphate Dependent Histidine Decarboxylase from *Morganella morganii*<sup>†</sup>

Lynn M. Abell and Marion H. O'Leary\*

Departments of Chemistry and Biochemistry, University of Wisconsin—Madison, Madison, Wisconsin 53706

Received December 22, 1987; Revised Manuscript Received April 12, 1988

**ABSTRACT:** The pyridoxal 5'-phosphate dependent histidine decarboxylase from *Morganella morganii* shows a nitrogen isotope effect  $k^{14}/k^{15} = 0.9770 \pm 0.0021$ , a carbon isotope effect  $k^{12}/k^{13} = 1.0308 \pm 0.0006$ , and a carbon isotope effect for L-[ $\alpha$ -<sup>2</sup>H]histidine of  $1.0333 \pm 0.0001$  at pH 6.3, 37 °C. These results indicate that the overall decarboxylation rate is limited jointly by the rate of Schiff base interchange and by the rate of decarboxylation. Although the observed isotope effects are quite different from those for the analogous glutamate decarboxylase from *Escherichia coli* [Abell, L. M., & O'Leary, M. H. (1988) *Biochemistry* 27, 3325], the intrinsic isotope effects for the two enzymes are essentially the same. The difference in observed isotope effects occurs because of a roughly twofold difference in the partitioning of the pyridoxal 5'-phosphate-substrate Schiff base between decarboxylation and Schiff base interchange. The observed nitrogen isotope effect requires that the imine nitrogen in this Schiff base is protonated. Comparison of carbon isotope effects for deuteriated and undeuteriated substrates reveals that the deuterium isotope effect on the decarboxylation step is about 1.20; thus, in the transition state for the decarboxylation step, the carbon-carbon bond is about two-thirds broken.

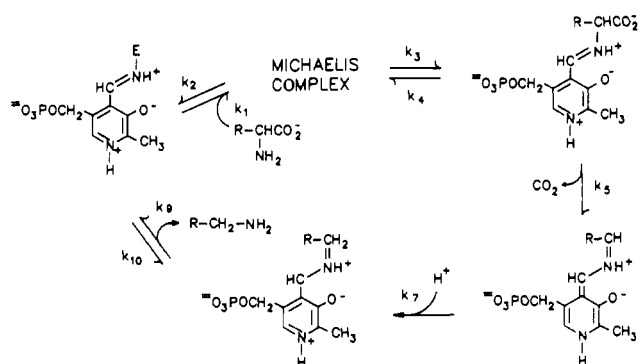
**P** yridoxal 5'-phosphate (PLP)<sup>1</sup> is the coenzyme for the majority of amino acid decarboxylases. The general mechanism by which these enzymes operate is well understood (Scheme I), and many aspects of this mechanism have been

studied (Boeker & Snell, 1972). A smaller class of amino acid decarboxylases lack PLP but contain instead a covalently

<sup>†</sup>This work was supported by Grants PCM 8216597 and DMB 8517501 from the National Science Foundation.

<sup>1</sup> Abbreviations: PLP, pyridoxal 5'-phosphate; HEPES, N-(2-hydroxyethyl)piperazine-N'-2-ethanesulfonic acid; MES, 2-(N-morpholino)ethanesulfonic acid; CHES, 3-(cyclohexylamino)ethanesulfonic acid.

Scheme 1



bound pyruvate that serves as a prosthetic group (Recsei & Snell, 1984). Enzymes in this latter category include decarboxylases for histidine, *S*-adenosylmethionine, and phosphatidyl serine. The proline reductase from *Clostridium sticklandii* also contains pyruvate and is the only pyruvoyl enzyme known to date that does not catalyze a decarboxylation (Recsei & Snell, 1984). The pyruvoyl decarboxylases operate by a mechanism formally similar to that of the PLP decarboxylases: Both mechanisms involve an imine (Schiff base) linkage between substrate and cofactor, and the cofactor serves as an electron sink in the decarboxylation step. Both classes of enzymes show high structural specificity and stereospecificity (Rosenthaler et al., 1965; Tanase et al., 1985).

It is interesting to speculate on the evolutionary relationship between the pyruvoyl system and the PLP system: Does the pyruvoyl system represent an evolutionary dead-end, in the sense that it is an imperfect way to catalyze decarboxylation, or is it simply an alternate, but equally efficient, method of solving the same problem? We were interested in gaining detailed kinetic information regarding each type of enzyme in order to answer this question.

Histidine decarboxylase is ideally suited for such a study because it is the only decarboxylase known to date that exists in both a PLP- and a pyruvate-dependent form. Both the PLP-dependent enzyme, which is the subject of this paper, and the pyruvoyl enzyme, which is the subject of the following paper (Abell & O'Leary, 1988b), have been extensively characterized by Snell and co-workers.

The PLP-dependent histidine decarboxylase from *Morganella morganii* AM-15 is a tetramer of identical subunits, each of  $M_r$  42 500. Each subunit binds 1 equiv of coenzyme. The existence of absorption bands at 416, 333, and 278 nm and the inactivation of the enzyme by NaCNBH<sub>3</sub> indicate that the coenzyme is bound to the enzyme by an imine linkage to a lysine residue. The amino acid sequence near this lysine residue shows sequence homology with other PLP-dependent decarboxylases (Tanase et al., 1985). The protein sequence has been determined, and the gene for histidine decarboxylase has also been identified and sequenced (Vaaler et al., 1986; E. E. Snell, private communication). There is no sequence homology between the pyruvoyl enzyme from *Lactobacillus* 30a and the PLP-dependent enzyme from *M. morganii*.

Kinetic properties of the PLP enzyme have been reported by Tanase et al. (1985). The enzyme has a pH optimum for both  $V_{max}$  and  $V_{max}/K_m$  near 6.5, and the activity decreases rather sharply on either side of the pH optimum. The enzyme is quite specific for histidine. Histamine, which is a potent competitive inhibitor of the pyruvoyl histidine decarboxylase, and methionine, which is a potent competitive inhibitor of the mammalian histidine decarboxylase, are very poor inhibitors of the enzyme from *M. morganii* (Tanase et al., 1985).

Our previous isotope effect studies of PLP-dependent decarboxylases provide a useful basis for the interpretation of isotope effects on histidine decarboxylase. Carbon isotope effects on PLP-dependent glutamate decarboxylase (O'Leary et al., 1970, 1981) and arginine decarboxylase (O'Leary & Piazza, 1978, 1981) are in the range  $k^{12}/k^{13} = 1.015\text{--}1.020$  for the natural substrates. Intrinsic isotope effects<sup>2</sup> are expected to be 1.05–1.06 (Marlier & O'Leary, 1986); thus, decarboxylation is only partially rate-determining. Nitrogen isotope effects on glutamate decarboxylase indicate that Schiff base interchange is also partially rate-determining and that the Schiff base nitrogen in the PLP–glutamate Schiff base intermediate is protonated [cf. Scheme I, Abell and O'Leary (1988a)].

Until recently, the magnitudes of heavy-atom isotope effects on enzymatic reactions were used simply to determine whether or not the isotope-sensitive step was rate-determining and to determine the ratio of rates for various steps. Recently, more sophisticated methods involving multiple isotope effects have been developed (Hermes et al., 1982). Such studies permit a higher level of definition of transition-state structure. This method has previously been applied to malic enzyme, which uses NAD as a cofactor (Hermes et al., 1982), formate dehydrogenase, which has no cofactor and works by a single-step mechanism (Hermes et al., 1984), and glutamate decarboxylase, which uses PLP (O'Leary et al., 1981).

The principle underlying these multiple isotope effect methods is that deuterium substitution in a substrate or in the solvent will change the rate of one or more steps in the reaction and that this change in turn will be reflected in heavy-atom isotope effects on the reaction. Deuterium substitution may decrease, increase, or not change the observed heavy-atom isotope effect, depending on the timing of the deuterium-sensitive step relative to the heavy-atom sensitive step (Hermes et al., 1982). In favorable cases, relatively unique intrinsic isotope effects can be obtained by this method, and from these intrinsic isotope effects, transition-state structures can be estimated.

In this paper we show that deuteration of the  $\alpha$ -carbon of an amino acid changes the carbon isotope effect on decarboxylation. This occurs as a result of the secondary isotope effect associated with the hybridization change in the transition state (Melander & Saunders, 1980). Comparison of carbon isotope effects with deuteriated and undeuteriated substrates provides a relatively unique set of intrinsic isotope effects for the overall reaction.

## MATERIALS AND METHODS

All chemicals were of reagent grade unless otherwise specified. Histidase from *Pseudomonas fluorescens*, porcine kidney acylase I, and glutamate dehydrogenase were obtained from Sigma Chemical Co. HEPES was obtained from United States Biochemical Corp. All other buffers were from Sigma. (Hydroxypropyl)cellulose was from Aldrich Chemical Co. Gold label grade D<sub>2</sub>O (<99.8% D) was obtained from Aldrich. Floropore ammonia-permeable membranes were from Millipore Corp. Amberlite IRC-50, analytical reagent grade, was converted to the H<sup>+</sup> form with 3 N acetic acid. The material was then washed well with water and adjusted to pH 7.0 with saturated LiOH and washed well with water. Dowex resin

<sup>2</sup> An intrinsic isotope effect is an isotope effect on an individual step in a multistep reaction mechanism. The observed isotope effect is related to the intrinsic isotope effect(s) by an equation involving a collection of terms of the form  $k_n/k_{n-1}$ .

was of analytical grade and was cleaned with bromine prior to use.

**PLP-Dependent Histidine Decarboxylase.** Histidine decarboxylase from *M. morganii* was prepared as described by Tanase et al. (1985) in Dr. E. E. Snell's laboratory at the University of Texas under the guidance of Dr. Beverly Guirard. The resulting enzyme produced a single band on slab gel electrophoresis and had a specific activity of  $70 \mu\text{mol of CO}_2 \text{ min}^{-1} (\text{mg of protein})^{-1}$ .

The enzyme was assayed manometrically at  $37^\circ\text{C}$  in a Gilson differential respirometer. The 2.5-mL assay solution contained 20 mM histidine, 200 mM MES, 0.01 mM PLP, 2.5 mM 2-mercaptoethanol, 0.09 mg/mL (hydroxypropyl)-cellulose, and 0.1 mM EDTA, pH 6.5 at  $25^\circ\text{C}$  (pH 6.3 at  $37^\circ\text{C}$ ). One sidearm of the Warburg flask contained 0.4 mL of buffer, and the other contained 0.1 mL of 10 N  $\text{H}_2\text{SO}_4$ . The enzyme was too unstable to withstand the complete incubation time of 30 min, so all components except enzyme were incubated for 25 min, at which time the enzyme was added to the sidearm containing buffer. Incubation was then carried out for another 5 min prior to the start of the reaction. The reaction was allowed to proceed for 10 min, and the reaction was quenched with the  $\text{H}_2\text{SO}_4$ . The total amount of  $\text{CO}_2$  released was corrected for the  $\text{CO}_2$  dissolved in the buffer by measuring the amount of  $\text{CO}_2$  released upon the addition of acid to a reaction mixture that did not contain enzyme.

### Synthesis

**DL- $[\alpha\text{-}^2\text{H}]$ -N-Acetylhistidine.** This synthesis was based on the method of Fujihara and Schowen (1984). Two grams of the free base of histidine was placed in a three-necked flask equipped with a condenser and an addition funnel and was dissolved in 10 mL of  $\text{D}_2\text{O}$  containing 2.1 M NaOD. The reaction mixture was cooled in an ice bath, and 20 mL of freshly distilled acetic anhydride was added dropwise. Upon completion of the addition, the ice bath was removed and replaced with an oil bath, and the reaction mixture was heated to  $55^\circ\text{C}$  under dry nitrogen for 20–24 h. The reaction mixture was then cooled with ice and 1.5 mL of concentrated  $\text{H}_2\text{SO}_4$  was added. The solution was then evaporated to dryness. The resulting solid was redissolved in water and evaporated to dryness. This procedure was repeated two more times. The solid was then dissolved in water and the pH adjusted to 7.0 with saturated LiOH. The solution was applied to an Amberlite IRC-50 column ( $45 \times 1.7 \text{ cm}$ ,  $\text{H}^+$  form). The column was eluted with water. The fractions were assayed for imidazole content by the Pauly test. Fractions that contained imidazole were combined and evaporated to dryness. Absolute ethanol (100 mL) was added to the solid, and the solution was refluxed for 1 h with stirring. The hot solution was then suction-filtered, and the filtrate was evaporated to dryness. The resulting solid was recrystallized from 70/30 acetone/water. The crystals were filtered, washed, and allowed to dry. A second crop of crystals was obtained by adding more acetone to the filtrate until it became cloudy. The solution was then kept at  $4^\circ\text{C}$  overnight while a second crop of crystals formed. The compound was characterized by  $^{13}\text{C}$  and  $^1\text{H}$  NMR. The extent of deuterium incorporation was determined by  $^1\text{H}$  NMR.

**L- $[\alpha\text{-}^2\text{H}]$ Histidine.** The resolution was carried out as described by Greenstein and Winitz (1974). One gram of racemic  $[\alpha\text{-}^2\text{H}]$ -N-acetylhistidine was dissolved in 50 mL of 0.1 M  $\text{NaP}_i$ , pH 7.4. Approximately 50 000 units of acylase I was added, and the reaction was allowed to proceed for 20 h at  $37^\circ\text{C}$  with agitation. Another 10 000 units of enzyme was added, and the reaction was allowed to proceed for another

20 h. The solution was then filtered through a PM-30 ultrafiltration membrane, and the pH was adjusted to 7.0. The solution was then applied to an Amberlite IRC-50 column ( $2.5 \times 40 \text{ cm}$ ,  $\text{H}^+$  form) at pH 7.0 and eluted first with water and then with 3 M acetic acid. Fractions containing imidazole were combined, and the volume was reduced by using a rotary evaporator. The concentrated solution was then placed on a Dowex 50W X-2 column ( $2.5 \times 40 \text{ cm}$ ,  $\text{H}^+$  form), which was then washed well with water. The column was eluted with 2 N  $\text{NH}_4\text{OH}$ . Fractions containing imidazole were combined and evaporated to dryness. The resulting solid was dissolved in a small amount of water and then lyophilized to dryness. Material from several resolutions was combined and recrystallized at this stage. The material was dissolved in a minimum of hot boiling water and then filtered hot. Boiling absolute ethanol was added until the solution turned cloudy (approximately 90% ethanol). The solution was allowed to cool slowly to room temperature and was kept at  $4^\circ\text{C}$  overnight. The crystals were filtered and washed with ethanol and then ether. The filtrate was evaporated to dryness and a second recrystallization performed. The specific rotation of the resolved material was  $-35.40$  [lit.  $-38.4$ ; Baker and Sober (1953)]. The material was also characterized by  $^1\text{H}$  and  $^{13}\text{C}$  NMR, and the extent of deuterium incorporation was found to be 94%.

### Methods

**Nitrogen Isotope Effects.** All glassware was washed with ammonia-free  $\text{H}_2\text{SO}_4$ , rinsed with water, and oven-dried prior to use. All solutions, including enzyme stock solutions, were tested for ammonia contamination prior to use by assaying with either Nessler's assay (Sigma) or glutamate dehydrogenase (Abell & O'Leary, 1988a).

Nitrogen isotope effects on histidine decarboxylase were measured by comparing the isotopic composition of the amino nitrogen of residual substrate after 50% or more reaction with the isotopic composition of the amino nitrogen in the initial substrate. Reactions were carried out at  $37^\circ\text{C}$ . Enzyme was prepared for these reactions by dialysis against 0.2 M MES buffer, pH 6.5. The reaction solutions contained 20 mM histidine in 200 mM MES, 0.01 mM PLP, 2.5 mM 2-mercaptoethanol, 0.09 mg/mL (hydroxypropyl)cellulose, and 0.1 mM EDTA, pH 6.5 at  $25^\circ\text{C}$  (at  $37^\circ\text{C}$ , the pH of this solution is 6.3). After the desired extent of reaction was reached, the reaction was quenched with 1.5 mL of 1 M  $\text{H}_2\text{SO}_4$ . The fraction reaction was calculated by isolating and measuring the amount of  $\text{CO}_2$  produced by continuous distillation. The isotopic composition of the amino nitrogen of histidine was selectively analyzed by deamination with histidine.

The reaction vessel used for deamination of histidine consisted of two glass compartments (volumes of 20 mL each) connected by an O-ring joint and an ammonia-permeable membrane. Both compartments were accessible via sidearms that were sealed with serum caps. Each compartment contained a 1-cm magnetic stirring bar.

The membrane was tested for leaks by filling one side with ammonia-free 50 mM  $\text{H}_2\text{SO}_4$  and the other with water. Both sides were stoppered and stirred 15 h. If the pH of the water remained unchanged, then the membrane was judged to be free of leaks and the reaction vessel was used for one deamination reaction. The membrane was found to be quite fragile and could be used for only one deamination reaction.

For deamination of histidine-containing solutions, one compartment contained 0.2 M CHES, pH 9, 2.5  $\mu\text{L}$  of 2-mercaptoethanol, 0.1 mM  $\text{MnCl}_2$ , and the histidine-containing reaction solution. The other side of the vessel contained 50

mM H<sub>2</sub>SO<sub>4</sub> and 25 mM NaCl in order to equalize the ionic strengths of both sides. Histidase (1000 units) was then added to the reaction side of the membrane vessel, and the deamination reaction was allowed to proceed at 25–30 °C with stirring for 24 h, after which another 500 units of histidase was added. The progress of the reaction was monitored by assaying for urocanate on the sample side by absorbance at 277 nm, for NH<sub>3</sub> on the sample side with glutamate dehydrogenase, and for NH<sub>3</sub> on the acid side with Nessler's reagent. When the reaction was complete, the ammonia was purified by steam distillation, the distillate was concentrated by evaporation, and the NH<sub>3</sub> solution was converted to N<sub>2</sub> with hypobromite as previously described (Abell & O'Leary, 1988a).

Control experiments using standard ammonia showed that the membrane did not fractionate isotopes, and the deamination reaction was shown to be complete by conducting several reactions in pyrophosphate buffer instead of CHES and then confirming the absence of remaining histidine by using the chromatography conditions described in the previous section on the resolution of DL-[α-<sup>2</sup>H]histidine. Isotope ratios were measured by using a Micromass 602E isotope ratio mass spectrometer at Washington University, St. Louis, MO, in the laboratory of Dr. Daniel Kohl.

Nitrogen isotope effects were calculated by using eq 1, where

$$k^{14}/k^{15} = \frac{\log(1-f)}{\log[(1-f)(R_s/R_0)]} \quad (1)$$

$R_s$  is the isotopic ratio of the position in the substrate after fraction reaction  $f$  and  $R_0$  is the isotopic ratio of that same position in the substrate prior to the reaction.

**Carbon Isotope Effects.** Carbon isotope effects were measured essentially as described by O'Leary (1980) by comparison of the isotopic content of CO<sub>2</sub> isolated after ca. 10% reaction with that of CO<sub>2</sub> isolated after 100% reaction. Reaction solutions contained 20 mM histidine (or 10 mM L-[α-<sup>2</sup>H]histidine), 200 mM MES, 0.01 mM PLP, 2.5 mM 2-mercaptoethanol, 0.09 mg/mL (hydroxypropyl)cellulose, and 0.1 mM EDTA, pH 6.3 at 25 °C (pH 6.3 at 37 °C).

CO<sub>2</sub> from all reactions was collected by a high-vacuum continuous distillation apparatus that utilized two dry ice–2-propanol traps and a liquid nitrogen trap and was purified further by three bulb-to-bulb distillations. The pressure in the vacuum line was kept around 200 mTorr throughout the distillation. A typical distillation required 30 min for completion. The volume of the resulting CO<sub>2</sub> was measured on a calibrated manometer in order to calculate the fraction reaction. CO<sub>2</sub> samples were analyzed by using a Finnigan Delta E isotope ratio mass spectrometer.

Control experiments were conducted for each set of carbon isotope effect conditions. One control experiment involved preparation of a reaction solution that contained all the reaction components except substrate, and the second involved preparation of a reaction solution that contained all components except enzyme. Each control was worked up in the usual manner to ensure that no extraneous CO<sub>2</sub> was produced in the absence of the enzymatic reaction.

Carbon isotope effects were calculated by using eq 2, where

$$k^{12}/k^{13} = \frac{\log(1-f)}{\log[1-f(R_p/R_0)]} \quad (2)$$

$R_p$  is the isotopic ratio of the product after fraction reaction  $f$  and  $R_0$  is the isotopic ratio of the product after complete reaction.

Table I: Carbon Isotope Effects on Histidine Decarboxylase from *M. organii* at pH 6.3, 37 °C, with H-Histidine

$\delta^{13}\text{C}$ (‰)			
complete conversion	low conversion	% reaction	$k^{12}/k^{13}$
-9.06 ± 0.02	-37.84 ± 0.03	6.7	1.0309
-9.00 ± 0.02	-38.21 ± 0.01	7.0	1.0315
-8.99 ± 0.01	-38.21 ± 0.02	2.8	1.0308
-8.99 ± 0.01	-37.28 ± 0.01	3.2	1.0299
-8.97 ± 0.01	-38.33 ± 0.02	3.4	1.0310
-9.00 <sup>a</sup>	-37.84 ± 0.01	3.2	1.0304
av 1.0308 ± 0.0006			
<sup>a</sup> Estimated from average of other 100% determinations.			

Table II: Carbon Isotope Effects on Histidine Decarboxylase from *M. organii* with [α-<sup>2</sup>H]Histidine at pH 6.3, 37 °C<sup>a</sup>

$\delta^{13}\text{C}$ (‰)	% reaction	$k^{12}/k^{13}$
-37.12 ± 0.03	9.3	1.0332
-37.10 ± 0.03	9.4	1.0332
-36.95 ± 0.03	10.3	1.0332
-36.71 ± 0.02	11.4	1.0331
-35.52 ± 0.02	18.0	1.0330
-35.16 ± 0.03	20.6	1.0332
-6.513 ± 0.031	100	
-6.909 ± 0.029	100	
av 1.0331 ± 0.0001		

<sup>a</sup> All isotope effects were calculated by using an average  $\delta^{13}\text{C}$  value for the 100% reaction samples of -6.710 ‰ (Abell & O'Leary, 1988b).

Isotope ratios for both carbon and nitrogen are reported as  $\delta^{15}\text{N}$  or  $\delta^{13}\text{C}$  defined by eq 3, where  $R_{\text{sp}}/R_{\text{std}}$  are isotope

$$\delta^{15}\text{N} \text{ or } \delta^{13}\text{C} = (R_{\text{sp}}/R_{\text{std}} - 1) \times 10^3 \quad (3)$$

ratios  $^{14}\text{N}^{15}\text{N}/^{14}\text{N}_2$  or  $^{13}\text{CO}_2/^{12}\text{CO}_2$  for sample and standard, respectively. The standard for nitrogen is air, and that for carbon is PDB limestone.

## RESULTS

Carbon isotope effects on the decarboxylation of histidine by histidine decarboxylase from *M. organii* are summarized in Table I. The isotope effects were calculated in a pairwise fashion by using eq 2. The isotopic content of CO<sub>2</sub> from the 100% reaction samples was in good agreement with the values obtained with the enzyme from *Lactobacillus* 30a (Abell & O'Leary, 1988b), which were obtained with the same batch of histidine.

A similar set of isotope effects using L-[α-<sup>2</sup>H]histidine are summarized in Table II. Since the extent of deuterium incorporation in the labeled substrate was 94% as determined by NMR, the observed isotope effect of 1.0331 is only 94% of the actual isotope effect. When the isotope effect is corrected for the extent of deuterium incorporation, the value becomes 1.0333. Only two complete decarboxylation reactions were carried out; however, the  $\delta^{13}\text{C}$  value of -6.711 ± 0.280 obtained for the CO<sub>2</sub> from these two reactions is in good agreement with the  $\delta^{13}\text{C}$  value of -6.670 ± 0.168 measured for the complete decarboxylation reactions carried out with pyruvoyl histidine decarboxylase (see accompanying paper) on the same L-[α-<sup>2</sup>H]histidine.

Nitrogen isotope effects were measured by comparing the isotopic composition of the amino nitrogen of histidine remaining after partial decarboxylation with that of the starting histidine. The amino nitrogen was selectively isolated by deamination with histidase using an ammonia-permeable membrane to drive the reaction to completion. The results of nitrogen isotope effect measurements are given in Table III.

Table III: Nitrogen Isotope Effects on Histidine Decarboxylase from *M. morganii* at pH 6.3, 37 °C

$\delta^{15}\text{N}$ (‰)	% reaction	$k^{14}/k^{15}$
12.53 ± 0.05	100	
14.10 ± 0.03	100	
14.19 ± 0.06	100	
av 13.60 ± 0.93		
9.05 ± 0.05	42	0.9919
8.31 ± 0.02	42	0.9905
10.09 ± 0.04	42	0.9937
8.48 ± 0.03	50	0.9928
9.01 ± 0.04	42	0.9917
10.13 ± 0.05	33	0.9914
9.36 ± 0.07	55	0.9948
8.47 ± 0.05	59	0.9944
8.03 ± 0.07	63	0.9945
9.26 ± 0.04	51	0.9958
av 0.9931 ± 0.0020		

The calculated values in the last column of Table III are isotope effects relative to protonated (i.e.,  $-\text{NH}_3^+$ ) histidine as the starting state. These values can be corrected to the unprotonated value by dividing by the equilibrium nitrogen isotope effect reported by Hermes et al. (1985) for the protonation-deprotonation equilibrium of phenylalanine (1.0165). The isotope effect compared to unprotonated histidine thus becomes 0.9770.

## DISCUSSION

Carbon isotope effects for the PLP-dependent glutamate and arginine decarboxylases are 1.015–1.020 at the optimum pH for the natural substrate (O'Leary et al., 1970, 1981; O'Leary & Piazza, 1981). Intrinsic carbon isotope effects are expected to be in the range 1.05–1.06 (Marlier & O'Leary, 1986), and these smaller isotope effects are interpreted as being due to decarboxylation and Schiff base interchange being jointly rate-determining. Nitrogen isotope effects on glutamate decarboxylase are consistent with this conclusion and eliminate the alternate possibility that the small carbon isotope effects are due to partially rate-determining substrate binding or conformation change associated with substrate binding (Abell & O'Leary, 1988a). The carbon isotope effect of 1.031 observed with the PLP-dependent histidine decarboxylase is significantly larger than values observed previously and indicates that the decarboxylation step is more nearly rate-determining in this case than in previous cases.

Deuteration of histidine increases the carbon isotope effect from  $1.0308 \pm 0.0006$  to  $1.0333 \pm 0.0001$ . This change can be understood from the treatment developed by Hermes et al. (1982). Qualitatively, the fact that deuteration of the substrate increases the carbon isotope effect indicates that the deuterium-sensitive step and the carbon-13-sensitive step are the same. Deuteration is expected to decrease the rate of the decarboxylation step, but not to have effects on rates of preceding steps. Consequently, the decarboxylation step becomes slightly more rate-determining, and the carbon isotope effect increases.

Not only is the carbon isotope effect significantly different in this case from that in previous cases, but the nitrogen isotope effect is as well (0.977 for histidine decarboxylase vs 0.985 for glutamate decarboxylase). The question to be addressed here is what differences between these enzymes are responsible for the differences in isotope effects. The carbon isotope effect observed with deuterated substrate will allow a more thorough interpretation of the heavy-atom isotope effects measured for the PLP-dependent histidine decarboxylase than has been

Table IV: Calculated Rate Ratios  $k_5/k_4$ , Intrinsic Hydrogen and Intrinsic Nitrogen Isotope Effects for the Decarboxylation of Histidine by the PLP-Dependent Histidine Decarboxylase from *M. morganii* at pH 6.3, 37 °C

derived parameter	assumed value of $k_5^{12}/k_5^{13}$	
	1.05	1.06
$k_5/k_4$	0.623	0.94
$k_5^{\text{H}}/k_5^{\text{D}}$	1.24	1.18
assumed $K^{14}/K^{15}$	0.9824, 0.9669	0.9824, 0.9669
$k_3^{14}/k_3^{15}$	0.9684, 0.9933	0.9716, 0.9872
$k_4^{14}/k_4^{15}$	0.9858, 1.0273	0.9890, 1.0210

possible in past studies of PLP-dependent decarboxylases.

**Quantitative Analysis of Isotope Effects.** For the mechanism of Scheme I, the carbon isotope effect on the enzymatic decarboxylation of histidine is given by eq 4, the nitrogen

$$k^{12}/k^{13} = \frac{k_5^{12}/k_5^{13} + k_5/k_4}{1 + k_5/k_4} \quad (4)$$

$$k^{14}/k^{15} = \frac{K_{\text{eq}}^{14}/K_{\text{eq}}^{15} + (k_3^{14}/k_3^{15})(k_5/k_4)}{1 + k_5/k_4} \quad (5)$$

$$k^{12}/k^{13} (\text{D}) = \frac{k_5^{12}/k_5^{13} + (k_5/k_4)/(k_5^{\text{H}}/k_5^{\text{D}})}{1 + (k_5/k_4)/(k_5^{\text{H}}/k_5^{\text{D}})} \quad (6)$$

isotope effect on the reaction by eq 5, and the carbon isotope effect for deuterated substrate by eq 6. The rate constants are those of Scheme I:  $K^{14}/K^{15}$  is the equilibrium isotope effect on Schiff base formation,  $k_5^{12}/k_5^{13}$  is the intrinsic carbon isotope effect on  $k_5$ ,  $k_3^{14}/k_3^{15}$  is the intrinsic nitrogen isotope effect on  $k_3$ , and  $k_5^{\text{H}}/k_5^{\text{D}}$  is the secondary deuterium isotope effect on  $k_5$ .

Implicit in eq 4–6 are several assumptions: First, substrate binding is at equilibrium; nitrogen and carbon isotope effect studies for this enzyme and for glutamate decarboxylase (Abell & O'Leary, 1988a) provide excellent evidence for this assumption. Second, only  $k_5$  shows a significant carbon isotope effect. Third, only  $k_3$  and  $k_4$  show significant nitrogen isotope effects. Fourth, only  $k_5$  shows a significant deuterium isotope effect. Finally, the intrinsic carbon isotope effects for deuterated and undeuterated substrates are the same. This last assumption is a consequence of the rule of the geometric mean (Bigeleisen, 1955) and should be true for present purposes.

**Carbon Isotope Effects.** Previous work allows us to limit our consideration of possible values for the intrinsic carbon isotope effect to the range 1.05–1.06 (Marlier & O'Leary, 1986). From this we can use eq 4 to estimate a value for  $k_5/k_4$  (Table IV) of 0.6–1.0. In previous cases this value was near 2, so decarboxylation is clearly more rate-determining in this case than in previous cases. Energetically, this is a small difference from the previous cases, reflecting a change of less than 1 kcal/mol in relative transition-state energies, but it is sufficiently large to make a substantial change in the observed isotope effects.

**Deuterium Isotope Effects.** Intrinsic secondary deuterium isotope effects such as that for L-[ $\alpha$ - $^2\text{H}$ ]histidine reflect the change in hybridization of the attached carbon on going from ground state to transition state. In the present case, the secondary deuterium isotope effect also reflects the rate ratio  $k_5/k_4$ . If an accurate value were available for the measured deuterium isotope effect on  $V_{\text{max}}/K_{\text{m}}$ , then we would be able to use the value of  $k_5/k_4$  obtained from the carbon isotope effect (cf. Table IV) to calculate a value for the intrinsic deuterium isotope effect. This value could be used to determine something about transition-state structure for the de-

Table V: Comparison of Kinetic Parameters for the PLP-Dependent Glutamate Decarboxylase and Histidine Decarboxylase under Optimum Conditions at 37 °C

	glutamate decarboxylase <sup>a</sup>	histidine decarboxylase <sup>b</sup>
obsd carbon isotope effect	1.018	1.031
obsd nitrogen isotope effect	0.985	0.977
derived $k_5/k_4$	1.7–2.3	0.6–1.0
$k_5^{12}/k_5^{13}$ <sup>c</sup>	1.05–1.06	1.05–1.06
$k_3^{14}/k_3^{15}$	0.993–0.996	0.987–0.993
$k_4^{14}/k_4^{15}$	1.028–1.030	1.021–1.027

<sup>a</sup> At pH 4.7. Data from Abell and O'Leary (1988a). <sup>b</sup> This work. <sup>c</sup> Assumed, on the basis of Marlier and O'Leary (1986).

carboxylation step. Unfortunately, the noncontinuous assay method used for the PLP-dependent histidine decarboxylase militates against obtaining an accurate measurement of this small secondary deuterium isotope effect.

An alternate method is available for obtaining the deuterium isotope effect. The carbon isotope effects for histidine and L-[ $\alpha$ -<sup>2</sup>H]histidine are different because of the hydrogen isotope effect on  $k_5$  (cf. eq 4 and 6). As shown in Table IV, the intrinsic carbon isotope effect can be estimated within narrow limits, from which a narrow range of values can be obtained for  $k_5/k_4$ . This ratio refers to substrate containing <sup>12</sup>C and <sup>1</sup>H and can be used in connection with eq 6 to obtain a value for  $k_5^H/k_5^D$ . As shown in Table IV, this value is  $1.20 \pm 0.05$ .

The value for  $k_5^H/k_5^D$  is expected to be close to 1.29 (the equilibrium isotope effect for a deuterium attached to a carbon that changes hybridization from sp<sup>3</sup> to sp<sup>2</sup>) if the transition state is product-like (Melander & Saunders, 1980), and the isotope effect is a monotonic (though not necessarily linear) function of hybridization. A hydrogen isotope effect of 1.20 indicates that the carbon–carbon bond is substantially broken in the transition state.

**Nitrogen Isotope Effects.** Values for  $k_5/k_4$  that were obtained from the carbon isotope effects (eq 4, Table IV) can be used together with the known equilibrium isotope effect on Schiff base formation (Abell & O'Leary, 1988a) to calculate intrinsic nitrogen isotope effects on  $k_3$  and  $k_4$ . Two possible values for the equilibrium isotope effect may be used in these calculations, depending on whether we assume the nitrogen in the substrate–Schiff base intermediate is protonated (0.9669) or unprotonated (0.9824). The results of these calculations for the two possible values of the equilibrium isotope effect are shown in the last two lines of Table IV.

When the assumed equilibrium isotope effect is that for unprotonated Schiff base (0.9824), the nitrogen isotope effects on both  $k_3$  and  $k_4$  are inverse. As we have noted previously (Abell & O'Leary, 1988a), an inverse isotope effect on  $k_3$  is theoretically possible, though to our knowledge no experimental precedents exist. However, an inverse isotope effect on  $k_4$  is not possible. This step represents a bond-breaking reaction, and such reactions should have significant normal isotope effects. Thus, we conclude that intrinsic isotope effects derived from the unprotonated Schiff base model are inconsistent with our expectations.

When the assumed equilibrium isotope effect is that for the protonated Schiff base (0.9669), the nitrogen isotope effect calculated for  $k_3$  is slightly inverse, whereas the nitrogen isotope effect on  $k_4$  is normal. Analogy with other C–N bond-breaking reactions suggests that the nitrogen isotope effect on  $k_4$  should be near 1.02–1.03 (Abell & O'Leary, 1988a). The isotope effect on  $k_4$ , in particular, is 1.021 or 1.027, depending on the assumed value of the intrinsic carbon

isotope effect on  $k_5$ , and these values are nicely within the range expected for such effects. Thus, we conclude that the substrate–Schiff base intermediate is protonated and that this last set of intrinsic isotope effects is the correct one.

**Comparison with Glutamate Decarboxylase.** It is interesting to compare the results of this analysis with the corresponding results for the PLP-dependent glutamate decarboxylase (Abell & O'Leary, 1988a). Appropriate comparisons are summarized in Table V, on the basis of the best values of the isotope effects for the two enzymes.

The observed carbon and nitrogen isotope effects are quite different. However, this does not reflect any significant difference in mechanism or in intrinsic isotope effects; rather, it is simply a manifestation of a roughly twofold difference in the rate ratio  $k_5/k_4$ , which reflects the partitioning of the PLP–substrate Schiff base intermediate. The difference in the ratio  $k_5/k_4$  for these two enzymes indicates that Schiff base formation is slightly more rate-limiting than decarboxylation in the case of glutamate decarboxylase, whereas decarboxylation is slightly more rate-limiting for histidine decarboxylase. In both cases, the energy difference between the two transition states is less than 1 kcal/mol. The nitrogen isotope effects require that the intermediate Schiff base nitrogen is protonated in both enzymes. Calculated intrinsic nitrogen isotope effects are inconsistent with the possibility that the Schiff base is unprotonated.

Although deuterium isotope effects have not been previously measured on other PLP-dependent decarboxylases, the use of deuterium isotope effects on carbon isotope effects in the case of histidine decarboxylase demonstrates that this method is useful particularly in cases where the direct measurement of deuterium isotope effects is impractical. The deuterium isotope effect indicates that the transition state for the decarboxylation is rather late. This conclusion has not been available from carbon isotope effects, because previous work does not enable us to predict how the intrinsic carbon isotope effect on such a reaction might vary as a function of degree of C–C bond breaking in the transition state.

#### ACKNOWLEDGMENTS

We thank Dr. E. E. Snell and Dr. Beverly Guirard for help in the isolation of PLP-dependent histidine decarboxylase, Dr. Daniel Kohl and Dr. Georgia Shearer for assistance with nitrogen isotope ratio measurements, and Dr. Paul Weiss for his advice concerning nitrogen analyses.

#### REFERENCES

- Abell, L. M., & O'Leary, M. H. (1988a) *Biochemistry* 27, 3325.
- Abell, L. M., & O'Leary, M. H. (1988b) *Biochemistry* (following paper in this issue).
- Baker, C. G., & Sober, H. A. (1953) *J. Am. Chem. Soc.* 75, 4058.
- Bigeleisen, J. (1955) *J. Chem. Phys.* 23, 2264.
- Boeker, E. A., & Snell, E. E. (1972) *Enzymes* (3rd Ed.) 6, 217.
- Fujiyara, H., & Schowen, R. L. (1984) *J. Org. Chem.* 49, 2819.
- Greenstein, J. P., & Winitz, M. (1974) *Chemistry of the Amino Acids* Vol. 1, p 63, Wiley, New York.
- Hermes, J. D., Roeske, C. A., O'Leary, M. H., & Cleland, W. W. (1982) *Biochemistry* 21, 5106.
- Hermes, J. D., Morrical, S. W., O'Leary, M. H., & Cleland, W. W. (1984) *Biochemistry* 23, 5479.
- Hermes, J. D., Weiss, P. M., & Cleland, W. W. (1985) *Biochemistry* 24, 2959.

- Marlier, J. F., & O'Leary, M. H. (1986) *J. Am. Chem. Soc.* 108, 4896.
- Marburg, S., Duggan, D. E., Maycock, A. L., & Aster, S. D. (1978) *Nature (London)* 274, 906.
- Melander, L., & Saunders, W. H. (1980) *Reaction Rates of Isotopic Molecules*, Wiley, New York.
- O'Leary, M. H. (1980) *Methods Enzymol.* 83, 64.
- O'Leary, M. H., & Piazza, G. J. (1978) *J. Am. Chem. Soc.* 100, 632.
- O'Leary, M. H., & Piazza, G. J. (1981) *Biochemistry* 20, 2743.
- O'Leary, M. H., Richards, D. T., & Hendrickson, D. W. (1970) *J. Am. Chem. Soc.* 92, 4435.
- O'Leary, M. H., Yamada, H., & Yapp, C. J. (1981) *Biochemistry* 20, 1476.
- Recsei, P., & Snell, E. E. (1984) *Annu. Rev. Biochem.* 53, 357.
- Rosenthaler, J., Guirard, B. M., Chang, G. W., & Snell, E. E. (1965) *Proc. Natl. Acad. Sci. U.S.A.* 54, 152.
- Tanase, S., Guirard, B. M., & Snell, E. E. (1985) *J. Biol. Chem.* 260, 6738.
- Vaaler, G. L., Brasch, M. A., & Snell, E. E. (1986) *J. Biol. Chem.* 261, 11010.
- Wada, H., Watanabe, T., Maeyama, K., Taguchi, Y., & Hayashi, H. (1984) in *Chemical and Biological Aspects of Vitamin B<sub>6</sub> Catalysis, Part A* (Evangelopoulos, A. E., Ed.) p 245, Alan R. Liss, New York.

## Isotope Effect Studies of the Pyruvate-Dependent Histidine Decarboxylase from *Lactobacillus* 30a<sup>†</sup>

Lynn M. Abell and Marion H. O'Leary\*

Departments of Chemistry and Biochemistry, University of Wisconsin—Madison, Madison, Wisconsin 53706

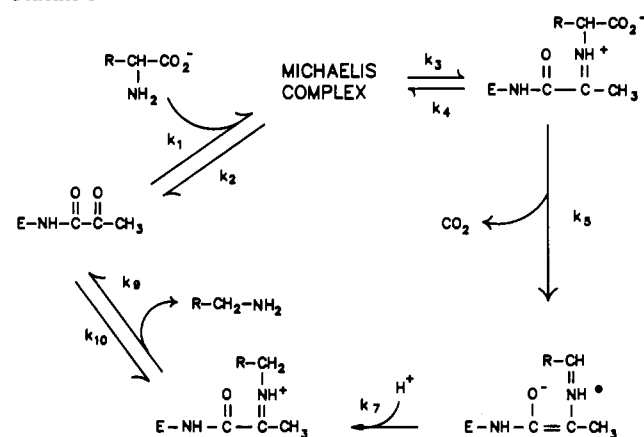
Received December 22, 1987; Revised Manuscript Received April 12, 1988

**ABSTRACT:** The decarboxylation of histidine by the pyruvate-dependent histidine decarboxylase of *Lactobacillus* 30a shows a carbon isotope effect  $k^{12}/k^{13} = 1.0334 \pm 0.0005$  and a nitrogen isotope effect  $k^{14}/k^{15} = 0.9799 \pm 0.0006$  at pH 4.8, 37 °C. The carbon isotope effect is slightly increased by deuteration of the substrate and slightly decreased in D<sub>2</sub>O. The observed nitrogen isotope effect indicates that the imine nitrogen in the substrate-Schiff base intermediate complex is ordinarily protonated, and the pH dependence of the carbon isotope effect indicates that both protonated and unprotonated forms of this intermediate are capable of undergoing decarboxylation. As with the pyridoxal 5'-phosphate dependent enzyme, Schiff base formation and decarboxylation are jointly rate-limiting, with the intermediate histidine-pyruvate Schiff base showing a decarboxylation/Schiff base hydrolysis ratio of 0.5–1.0 at pH 4.8. The decarboxylation transition state is more reactant-like for the pyruvate-dependent enzyme than for the pyridoxal 5'-phosphate dependent enzyme. These studies find no particular energetic or catalytic advantage to the use of pyridoxal 5'-phosphate over covalently bound pyruvate in catalysis of the decarboxylation of histidine.

In 1953, Rodwell discovered that the Gram-positive bacterium *Lactobacillus* 30a contained a large quantity of histidine decarboxylase (Rodwell, 1953). Closer examination of the properties of this enzyme by Rosenthaler et al. (1965) confirmed Rodwell's suspicion that this particular histidine decarboxylase did not require the cofactor pyridoxal 5'-phosphate (PLP)<sup>1</sup> for catalysis. Instead, the enzyme contains a covalently bound pyruvoyl residue as its prosthetic group (Riley & Snell, 1968). Subsequent studies have revealed the existence of a small class of enzymes, principally decarboxylases, that require covalently bound pyruvate for catalysis, rather than the more common PLP (Recsei & Snell, 1984). The mechanistic comparison of these two classes of enzymes is the subject of the present study.

The pyruvate-dependent histidine decarboxylase from *Lactobacillus* 30a contains covalently bound pyruvate, but contains no metal ion or other cofactors. The enzyme has a molecular weight of 208 000 and a hexameric subunit structure ( $\alpha\beta$ )<sub>6</sub> (Hackert et al., 1981). The hexamer contains six active sites and one pyruvoyl residue per active site. The larger  $\alpha$  subunit contains the pyruvoyl residue, which is covalently bound to the amino-terminal phenylalanine. The smaller  $\beta$  subunit, which is essential for activity, does not contain pyruvate,

Scheme I



or cysteine, histidine, or phenylalanine (Huynh et al., 1984). A 3-Å X-ray crystal structure of this enzyme (Hackert et al., 1981; Parks et al., 1985) shows that lysine-155 and a glutamic acid are present in the active site, which is at the bottom of a deep cleft. Modification of lysine-155 with

<sup>†</sup> This work was supported by Grants PCM 8216597 and DMB 8517501 from the National Science Foundation.

<sup>1</sup> Abbreviations: PLP, pyridoxal 5'-phosphate; HEPES, N-(2-hydroxyethyl)piperazine-N'-2-ethanesulfonic acid; MES, 2-(N-morpholino)ethanesulfonic acid; CHES, 3-(cyclohexylamino)ethanesulfonic acid.